

# Wide-Band Suppression of Laser Intensity Noise

E. N. Ivanov and L. Hollberg

**Abstract** - A wide-band power control system based on an electro-optical modulator and transimpedance amplifier has been constructed. It is capable of reducing laser intensity fluctuations to the shot noise limit over the range of Fourier frequencies from a few tens of *Hz* to a few *MHz* with the low boundary set by the light handling capacity of a photodetector and the upper boundary imposed by the spurious resonances of a given electro-optical modulator. We discuss a general approach to the design of laser intensity control system and its noise properties.

**Index Terms** – noise spectral density, feedback control, shot noise

## I. Introduction

High power, low noise lasers are required for a wide range of metrological applications including the detection of gravitational waves and precision measurements of optical frequencies [1-3]. In the latter case, the ultra-precise measurements of optical frequencies were performed with mode-locked femtosecond lasers capable of generating extremely broad spectra of equidistant modes (optical combs) [4, 5]. Using such lasers it is also possible to convert the light-wave output of an optical “clock” into ultra-stable microwave signal [6]. This is achieved by synchronizing the pulse repetition rate of a femtosecond laser with a beat rate of an optical “clock” and detecting the optical pulse train with a high-speed photodetector. Phase synchronization of femtosecond lasers and demodulation of ultra-short light pulses is accompanied by excess phase noise [7]. One of the noise mechanisms contributing to the overall uncertainty of the frequency transfer between the optical and microwave domains is the intensity fluctuations of the pump laser driving the femtosecond comb generator. Reducing the pump laser intensity fluctuations is especially important for the development of the next generation of compact femtosecond laser systems based on low power, but often noisy, pump lasers. In this work we present the noise analysis of a wide-band laser intensity noise reduction system, discuss the noise mechanisms affecting its performance and summarize the steps one must take to ensure its stable operation.

## II. Noise Analysis

A schematic diagram of the laser intensity control system is shown in Fig. 1. It consists of a transverse-field electro-optical modulator (EOM), polarizer, trans-impedance (TI) amplifier and loop filter. A fraction of laser light passing through the EOM falls on a photodetector of a TI amplifier producing voltage proportional to the power of incident light. This voltage is compared with a stable reference at the input of TI-amplifier resulting in the difference (error) signal which is fed back to the EOM altering the power of the laser beam and keeping the error voltage close to zero.

The EOM and TI amplifier act, respectively, as an actuator and a sensor of the laser power control system. Below we derive the characteristic equation of the laser power control system and discuss the major noise mechanisms affecting its noise performance.

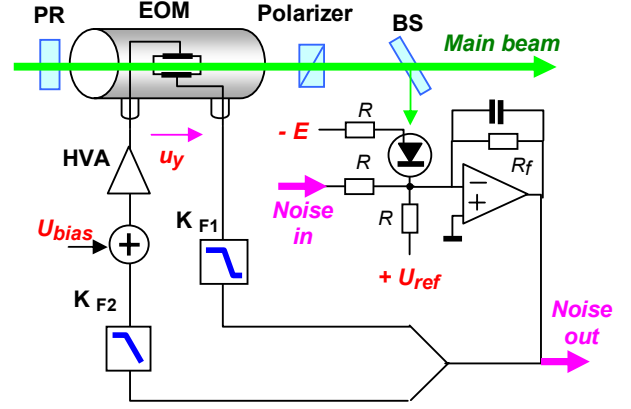


Fig. 1. Schematic diagram of a laser power control system: EOM – electro-optical modulator, PR – polarization rotator, BS – beam-splitter, HVA – high-voltage amplifier.

Power incident on a photodetector in Fig. 1 is given by

$$P_{det} = P_{inp} \alpha(u_y) k_{BS}, \quad (1)$$

where  $P_{inp}$  is the power of the input beam incident on the EOM,  $k_{BS}$  is the fraction of total laser power directed to the photodetector and  $\alpha$  is the insertion loss of EOM & polarizer assembly which depends on the EOM applied voltage  $u_y$ . The latter is the sum of a fixed term  $U_o$  (set manually to minimize the error signal before closing the loop) and a variable term representing the filtered error signal from the output of the TI-amplifier  $u_{amp}$ :

$$u_y = U_o + K_F(s) u_{amp}, \quad (2)$$

where  $K_F(s)$  is the differential operator characterizing the loop filter transfer function. In the case of a two-port EOM in Fig. 1:  $K_F = K_{F2} K_{HVA} - K_{F1}$ , where  $K_{F1}$ ,  $K_{F2}$  are the transfer functions of two filters in the EOM arms and  $K_{HVA}$  is the transfer function of the EOM high-voltage amplifier.

Assuming that the photodetector operates in a linear regime and ignoring limited bandwidth of the TI amplifier, the analytical expression for the voltage at the output TI amplifier can be presented as

$$u_{amp} = \eta R_f (P_{det} - \tilde{P}_{det}) \quad (3)$$

where  $\eta$  is the responsivity of the photodetector,  $R_f$  is the feedback resistor of the TI amplifier and  $\tilde{P}_{det}$  is the characteristic power which depends on the reference voltage  $U_{ref}$  at the input of the TI amplifier:  $\tilde{P}_{det} = U_{ref} / (\eta R_f)$ .

For rigorous calculations, the parameter  $R_f$  in (3) needs to be replaced with the differential operator  $\tilde{R}_f$  corresponding to the complex impedance of the TI amplifier:

$$\tilde{R}_f = \frac{1}{1/z_f + 1/(K_{amp} z_f) + sC/K_{amp}}, \quad (4)$$

where  $z_f$  is the feedback impedance of TI amplifier ( $z_f = R_f / (1 + s\tau)$ ,  $\tau$  is the time constant of the TI amplifier),  $C$  is the stray capacitance of a photodetector and  $K_{amp}$  is the open loop gain of the TI amplifier.

By substituting (2-4) into (1) and expanding the function  $\alpha(u_y)$  in Taylor series in the vicinity of  $U_o$ , a linearized characteristic equation of the power control system is obtained

$$P_{det} = P_{det}^{f/run} + S_y K_F(s) \eta \tilde{R}_f (P_{det} - \tilde{P}_{det}), \quad (5)$$

where  $P_{det}^{f/run} = P_{inp} \alpha(U_o) k_{BS}$  is the power incident on the photodetector with the control loop open and  $S_y = P_{inp} k_{BS} d\alpha/du_y$  is the conversion efficiency of the power actuator (for a typical EOM:  $\alpha(u_y) \sim \sin^2(u_y/V_{HW})$ , where  $V_{HW}$  is the EOM half-wave voltage, the maximum voltage-to-power conversion efficiency:  $S_y^{max} \approx 2P_{det}/V_{HW}$ ).

Power fluctuations in the laser beam incident on the photodetector  $\delta P_{det}$  can be found from (5) by assuming that all parameters of the power control system fluctuate around their mean values, for example:  $U_{ref} = \bar{U}_{ref} + \delta U_{ref}$ . Also, one has to account for the intrinsic noise of the TI amplifier  $\delta u_{amp}$ . An analytical expression for the  $\delta P_{det}$  is given by

$$\delta P_{det} = \frac{\delta P_{det}^{f/run}}{1 + \gamma} + \frac{\gamma}{1 + \gamma} \frac{(\delta U_{ref} + \delta u_{amp})}{\eta \tilde{R}_f} \quad (6)$$

where  $\delta P_{det}^{f/run}$  is the power fluctuations of a “free-running” laser (with the power control system switched off) and  $\gamma$  is the open loop gain ( $\gamma = -\eta \tilde{R}_f K_F S_y$ ).

Voltage noise at the output of TI amplifier  $\delta u_{amp}$  can be presented as a symbolic sum

$$\delta u_{amp} = \sqrt{8k_B T R_f} + \delta e_{amp} + \delta i_{amp} R_f + \sqrt{2q\eta P_{det}} R_f, \quad (7)$$

where  $k_B$  is the Boltzmann’s constant,  $T$  is the ambient temperature and  $q$  is the electron’s charge.

The first term in (7) describes the effect of thermal fluctuations in resistors of the TI amplifier (all resistors are assumed to be equal). The second and third terms in (7) represent, respectively, voltage and current fluctuations of the operational amplifier on which the TI amplifier is based. The last term in (7) results from the laser shot noise.

Following from (7), at high incident power  $P_{det}$  voltage fluctuations at the output of TI amplifier should be entirely due to the laser shot noise. Furthermore, assuming that  $|\gamma| \gg 1$  and making use of (6, 7), the analytical expression for the shot noise limited fluctuations  $\delta P_{det}$  can be obtained as:

$$\delta P_{det}^{shot} \approx \sqrt{2q P_{det} / \eta}, \quad (8)$$

Introducing an index of random amplitude modulation  $m = \delta P_{det} / (2P_{det})$ , the shot noise limited spectral density of relative intensity fluctuations (RIN) is expressed as:

$$S_m^{shot} = \frac{q}{2\eta P_{det}}. \quad (9)$$

For a typical set of parameters:  $\eta = 0.3 \text{ A/W}$  and  $P_{det} = 5 \text{ mW}$  equation (9) results in  $S_m^{shot} \approx -162 \text{ dBc/Hz}$ , which is  $\sim 17 \text{ dB}$  higher than the thermal noise limit (first term in eq. 7).

### III. Results and Discussion

The TI amplifier was implemented on a Si p-i-n photodetector S5973 (“Hamamatsu”) and high-speed operational amplifier AD8021 (“Analog Devices”)¹. It was built using surface-mount components and featured an auxiliary port for measuring its transfer function. Such a transfer function obtained with the RF network analyzer is shown in Fig. 2. To ensure a stable operation of the amplifier a  $0.2 \text{ pF}$  capacitor was inserted in the feedback

¹A specific product is named only for technical clarity and does not represent endorsement by the National Institute of Standards and Technology. Other products might be found to serve the purpose equally well.

path in parallel with the feedback resistor ( $R_f \approx 3k\Omega$ ). The bandwidth of the TI amplifier was found to be a diminishing function of input power  $P_{inp}$ . The largest bandwidth ( $\sim 130\text{ MHz}$ ) was measured in a small-signal regime at  $P_{inp} < -10\text{ dBm}$  (Fig. 2).

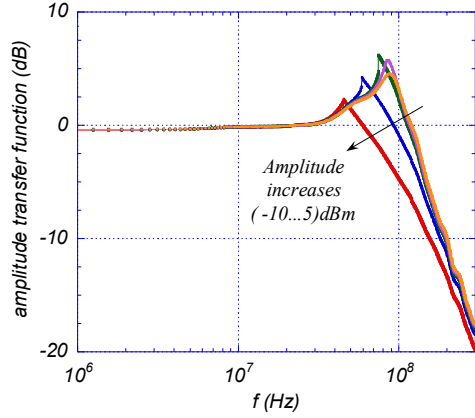


Fig. 2. Amplitude transfer function of trans-impedance amplifier at different levels of input RF signal

Fig. 3 shows spectra of voltage fluctuations at the output of TI amplifier measured with the light switched on and off (curves 1 and 2, respectively). In the latter case, the spectrum of the voltage fluctuations is the sum of  $1/f$  and “white” noise terms. The  $1/f$  noise dominates at low Fourier frequencies and results from the intrinsic fluctuations of the TI amplifier. The “white” noise is due to thermal fluctuations in the resistors (Johnson noise) of the TI amplifier. The horizontal line in Fig. 3 shows the shot noise contribution to the overall voltage fluctuations calculated at  $P_{det} = 1\text{ mW}$  (last term in eq. 7). At this level of power shot noise prevails in the spectrum of the TI amplifier voltage fluctuations at Fourier frequencies  $f > 500\text{ Hz}$ . By increasing the power incident on photodetector, one can extend the range of Fourier frequencies for which the sensitivity of the TI amplifier is shot noise limited. As a result, one can improve the quality of the power stabilization (see eq. 9).

A “tailored” loop filter is required to achieve the most broadband noise suppression without causing any noticeable noise enhancement outside the loop bandwidth. To design such a filter, one needs to know the complex transfer function for the optical assembly  $\gamma_{opt}$  formed by the EOM and TI amplifier, as the overall loop gain  $\gamma = \gamma_{opt} K_F$ .

Measurements of  $\gamma_{opt}$  were performed by varying the polarization of the laser light passing through the EOM. The induced power variations were detected with TI amplifier.

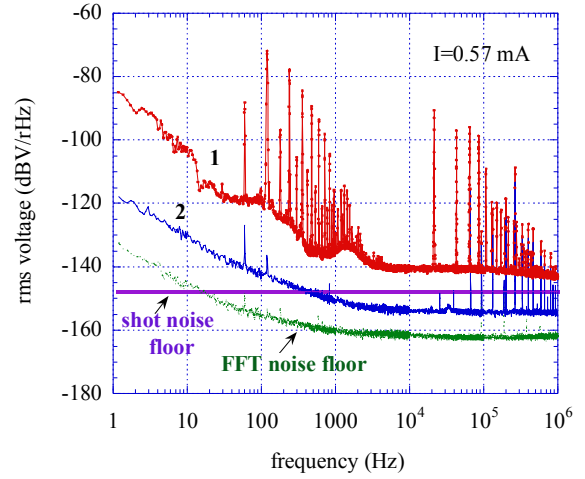


Fig. 3. Voltage noise spectra at the output of trans-impedance amplifier with the light switched on (curve 1) and off (curve 2). He-Ne laser was used as a light source, power incident on photodetector  $P_{det} \approx 1\text{ mW}$ .

During these measurements broadband voltage noise was injected into one input port of the EOM, while the other port was grounded. The amplitude transfer function of the “optical modem” is shown in Fig. 4. The average light power on the photodetector was  $\sim 1.5\text{ mW}$ . Two partially overlapping traces in Fig. 4 correspond to the data collected with different instruments: FFT spectrum analyzer and RF vector network analyzer.

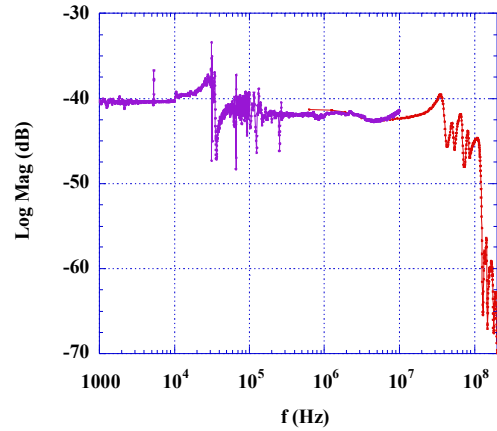


Fig. 4. Amplitude transfer function of “optical modem”.

In Fig. 4 the N-shaped distortion of the amplitude transfer function at frequencies around  $30\text{ kHz}$  is due to the piezo-mechanical resonance in the EOM crystal. This resonance, as was discovered later, did not affect the stability of the closed feedback loop. The “ripples” in the amplitude transfer function

$\gamma_{opt}$  at frequencies above  $20\text{ MHz}$  were linked to electrical resonances of the EOM.

While designing the loop filter we took advantage of the internal structure of the EOM with two floating inputs. This enabled us to split the error signal (see Fig. 1) and process separately its slow and fast fluctuations. The simulations were performed assuming that the “fast” arm of the filter was based on a AD8021 configured as an all-pass filter with a pole at  $100\text{ kHz}$  and a zero at  $50\text{ MHz}$ . The DC gain of the all-pass filter was designed to be  $60\text{ dB}$ . The “slow” arm of the loop filter was designed to include a “leaking integrator” (AD744) and a high-voltage amplifier (PA85 from “Apex Microtechnology”).

The filter design involved an analysis of loop stability, as well as calculations of the noise suppression factor  $N_s = I/(I + \gamma)$ . The latter is shown in Fig. 5 as a function of Fourier frequency at different levels of optical power. Results in Fig.5 are the best achievable for a chosen filter configuration.

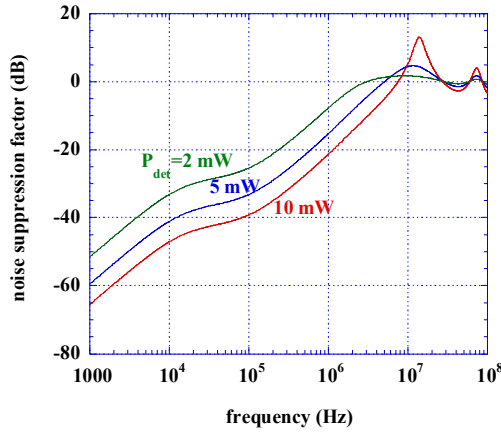


Fig. 5. Calculated noise suppression factor of laser power control system at different levels of power on photodetector.

The loop filter, like the TI amplifier, was implemented using surface-mount technology. The noise suppression factor of the power control system with the above filter is shown in Fig. 6. It was measured by injecting random noise to the auxiliary input port of the TI amplifier and monitoring its suppression at its output. Two traces in Fig. 6 correspond to the two different (by approximately a factor of 2) levels of laser power  $P_{inp}$ . In both cases the power incident on the photodetector  $P_{det}$  was set (by changing the EOM bias) close to  $7\text{ mW}$ . Data in Fig.6 indicates the bandwidth of the power control system is close to  $3...5\text{ MHz}$ .

Having a piezo-resonance in the EOM crystal at  $\sim 30\text{ kHz}$  did not compromise the loop stability. The above measurements were conducted with a  $532\text{ nm}$  laser “Verdi V8” (“Coherent”)

operating in a low power mode ( $P_{out} \approx 0.25\text{ W}$ ). This regime is characterized by excess intensity fluctuations, which results in the “fuzziness” of the experimental traces in Fig. 6.

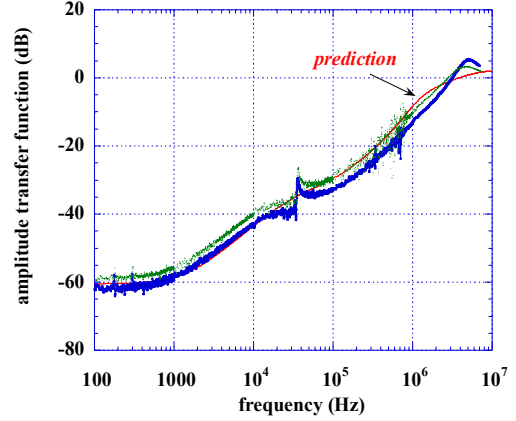


Fig. 6. Noise suppression factor of the power control system as a function of Fourier frequency at different levels of laser power

The observed lack of noise suppression at frequencies below  $1\text{ kHz}$  (relative to the results of calculations in Fig. 5) was due to the use of a low-pass filter ( $60\text{ dB}$  DC gain) instead of an integrator in the “slow” arm of the servo loop.

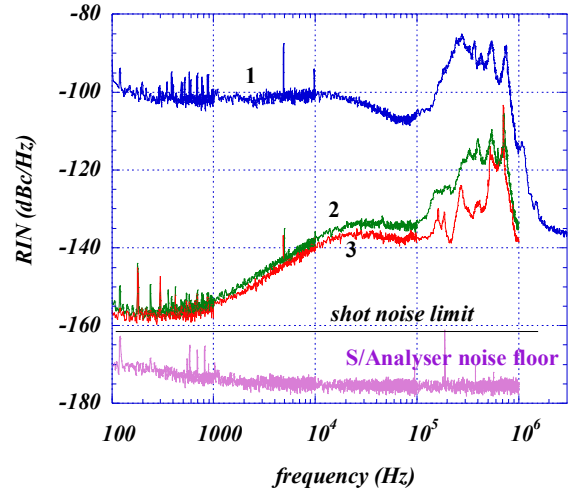


Fig. 7. Effect of the power control system on the spectral density of laser relative intensity fluctuations (in loop measurements with the “Verdi V8” laser operating in a low power mode). Detector power  $P_{det} \approx 7\text{ mW}$

Fig. 7 shows the effect of the power control system on the spectral density of the relative intensity fluctuations  $S_{RIN}$  of the laser light incident on the photodetector. The spectra in Fig.7

were inferred from the voltage noise at the output of TI amplifier via:

$$S_{RIN} = S_u / (2U_{DC})^2, \quad (10)$$

where  $S_u$  and  $U_{DC}$  are, respectively, the spectral density of the voltage fluctuations at the output of TI amplifier and its DC voltage. The observed noise cancellation at the output of TI amplifier with the control loop closed ( $\sim 60\text{ dB}$  at  $100\text{ Hz}$ ) was consistent with the noise suppression factor measured earlier (Fig. 6).

In a low power mode the intensity noise of a given laser was non-stationary. This explains the difference between the spectra 2, 3 (Fig. 7) which were taken a few minutes apart without any changes to the loop parameters or laser power. The horizontal line in Fig. 7 shows the shot noise limit for the spectral density of RIN at a given level of optical power  $P_{det}$ . With a small increase in loop gain, that may, for example, be introduced by an integrator in the “slow” arm of the control system, one could suppress laser power fluctuations to the shot noise limit at low Fourier frequencies

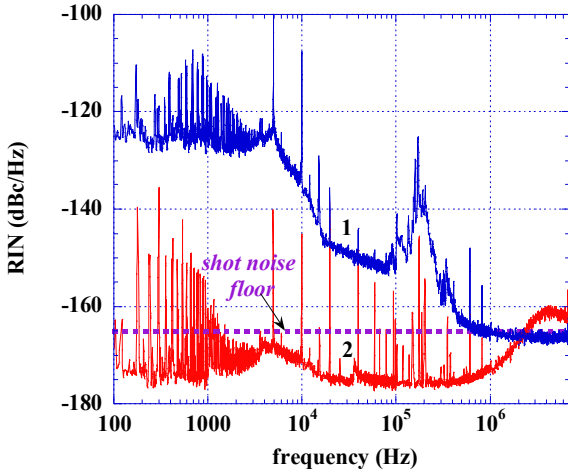


Fig. 8. Effect of the power control system on the spectral density of the laser relative intensity fluctuations (in-loop measurements with the “Verdi V8” laser operating in a high power mode).

Suppression of the laser amplitude noise to the shot noise limit was achieved with the “Verdi V8” laser working in a high power mode. This was due to more than  $20\text{ dB}$  reduction in laser intensity fluctuations associated with the increase in laser power (from  $0.25\text{ W}$  to  $9\text{ W}$ ). Fig. 8 shows the spectra of RIN of a “free-running” (curve 1) and power-stabilised laser (curve 2) at high output power. The latter spectrum was deduced from “in-loop” measurements of the voltage noise spectral density  $S_u$  in (10). The dash line in Fig. 8 corresponds to the shot noise limit at  $P_{det} \approx 9\text{ mW}$  (mean power on the photodetector was kept unchanged when laser power increased).

Remembering that the shot noise is a main contributor to the overall voltage fluctuations at the output of TI amplifier (Fig. 3), data in Fig. 8 show that the power control system is capable of suppressing the laser power fluctuations to the shot noise limit from a few tens of  $\text{Hz}$  up to a few  $\text{MHz}$ .

Splitting of the laser beam between the sensor of the power control system and the main beam (Fig. 1) adds an extra noise to the external signal. This noise results from the angular fluctuations of laser light incident on a beam splitter, as well as vibration of the beam-steering components and photodetectors [2, 7]. To characterize the noise properties of the external signal, laser light exiting the polarizer was split with a glass plate and sent to the additional (out of loop) TI amplifier.

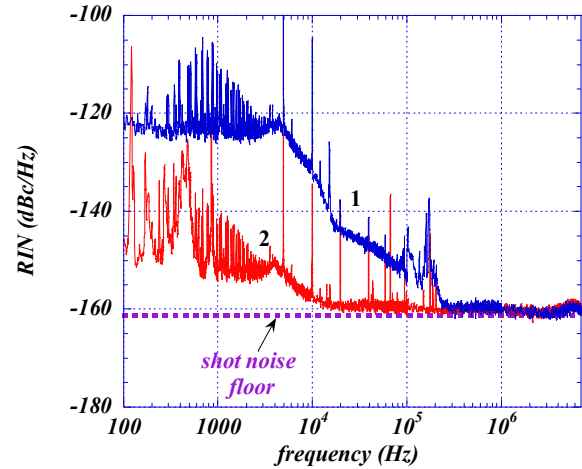


Fig. 9. Effect of power control system on spectral density of laser relative intensity noise (out of loop measurements with the “Verdi V8” laser operating in a high power mode).

The DC voltages at the output of the *in loop* and *out of loop* TI amplifiers were equal to  $6\text{ V}$  and  $3.5\text{ V}$ , respectively. Spectra of the RIN measured with the *out of loop* TI amplifier are shown in Fig. 9 (curves 1 and 2 correspond to the open and closed control loop, respectively). As follows from these results, power fluctuations of the external beam are shot noise limited at  $f > 10\text{ kHz}$ . At lower Fourier frequencies, the RIN of the external beam is higher than the shot noise limit. This indicates a presence of some additional noise in the spectrum of the external signal destroying the correlation between the power fluctuations in both beams. We speculate that the use of a fiber coupler or filtering of the beam angular fluctuations with a single mode fiber would eliminate this excess noise in the spectrum of the external signal [7, 8].

It’s worth mentioning a few simple steps one needs to follow to enable reliable locking of the power control system. First, one

has to “map” the voltage at the output of TI amplifier  $u_{amp}$  as a function of EOM bias  $u_y$ . This is required to ensure the proper sign of the feedback before closing the control loop. To conduct the voltage “mapping” the link between the TI amplifier and loop filter must be broken. To improve the “contrast” of the resulting dependence of  $u_{amp}$  on  $u_y$  the polarization of the laser light incident on the EOM is rotated relative to its crystal axis.

With no reference voltage applied to the input of the TI amplifier its output voltage  $u_{amp}$  remains positive for any values of EOM bias or laser power. To generate an error signal which changes its sign at the desired level of laser power, a positive reference voltage  $U_{ref}$  is added at the input of the TI amplifier. Typically, the level of  $U_{ref}$  is set to maximize the gradient  $du_{amp}/du_y$  at the zero-crossing point, if the associated insertion loss in the EOM ( $\sim 3\text{ dB}$ ) is tolerable. Finally, we found it is easier to acquire lock by closing the “fast” control loop first and then enabling the integrator. In this respect, it should be remembered that the sign of the voltage gradient  $du_{amp}/du_y$  at the zero-crossing point must be negative if the DC gain of the filter of the fast control loop  $K_{FI}$  is negative. This is because the overall loop gain of the power control system with the integrator disabled is:  $\gamma = -K_{FI} du_{amp}/du_y$ .

#### IV. Conclusion

A wide-band laser power stabilisation system capable of operating at the shot noise limit has been constructed. The bandwidth of the current system was limited to a few *MHz* due to the impedance mismatch of a given electro-optical modulator. We discuss: (i) a general approach to the design of power control systems; (ii) techniques for measuring the noise suppression factor of the feedback control system and (iii) possible reasons for the excess noise in the spectrum of the useful signal due to noise mechanisms other than power fluctuations.

#### V. Acknowledgement

Authors are grateful to R. Fox (NIST, Boulder, CO) for the assistance with the circuit design and J.-M. LeFloch (University of Western Australia) for proving the data acquisition software. This work is a collaboration between the University of Western Australia and the National Institute of Standards and Technology (Boulder, Colorado). It is supported by the Australian Research Council and the Defense Advanced Research Projects Agency.

#### References:

1. P. R. Saulson, “Interferometric gravitational wave detection: accomplishing the impossible”, *Class. Quantum Grav.* 17, pp. 2441-2448, 2000.
2. D. J. Ottaway, P. J. Veitch, C. Hollitt, D. Mudge, M. W. Hamilton and J. Munch, “Frequency and intensity noise of an injection-locked Nd:YAG ring laser”, *Appl. Phys B* 71, pp. 163-168, 2000.
3. Th. Udem, S. A. Diddams, K. R. Vogel, C. W. Oates, E. A. Curtis, W. D. Lee, W. M. Itano, R. E. Drullinger, J. C. Bergquist and L. Hollberg, “Absolute frequency measurements of the  $\text{Hg}^+$  and Ca optical clock transitions with a femtosecond laser”, *Phys. Rev. Letters*, vol. 86, p. 4996-4999, 2001.
4. J. L. Hall, J. Ye, S. A. Diddams, L. S. Ma, S. T. Cundiff and D. J. Jones, “Ultrasensitive Spectroscopy, the Ultrastable Lasers, and the Seriously Nonlinear Fiber: A New Alliance for Physics and Metrology”, *IEEE Journal of Quantum Electronics*, v. 37, no. 12, pp. 1482-1493, 2001.
5. L. Hollberg, C. W. Oates, E. A. Curtis, E. N. Ivanov, S. A. Diddams, Th. Udem, H. G. Robinson, J. C. Bergquist, R. J. Rafac, W. M. Itano, R. E. Drullinger and D. J. Wineland, “Optical Frequency Standards and Measurements”, *Journal of Quantum Electronics*, v. 37, no. 12, pp. 1502-1513, 2001.
6. J. J. McFerran, E. N. Ivanov, A. Bartels, G. Wilpers, C. W. Oates, S. A. Diddams, L. Hollberg, “Low-noise synthesis of microwave signals from an optical source”, *Electronics Letters*, vol. 41, issue 11, pp. 650-651, 26 May 2005.
7. E. N. Ivanov, S. A. Diddams and L. Hollberg, “Study of the Excess Noise Associated with Demodulation of Ultra-Short Infrared Pulses”, *IEEE Trans. on UFFC*, vol. 52, no. 7, pp. 1068-1075, 2005.
8. E. N. Ivanov, L. Hollberg and S. A. Diddams, “Analysis of Noise Mechanisms Limiting the Frequency Stability of Microwave Signals Generated with a Femtosecond Lasers”, *IEEE Journal of Selected Topics in Quantum Electronics*, vol. 9, no. 4, pp. 1059 - 1065, 2003.